



Article

The Metacaspase Gene *PoMCA1* Enhances the Mycelial Heat Stress Tolerance and Regulates the Fruiting Body Development of *Pleurotus ostreatus*

Jingqi Pei ^{1,2,3}, Mengran Zhao ^{2,3}, Lijiao Zhang ^{2,3} and Xiangli Wu ^{2,3,*}

¹ College of Food Science and Engineering, Shanxi Agricultural University, Jinzhong 030801, China; peijingqi666@163.com

² State Key Laboratory of Efficient Utilization of Arid and Semi-Arid Arable Land in Northern China, Institute of Agricultural Resources and Regional Planning, Chinese Academy of Agricultural Sciences, Beijing 100081, China; zhaomengran@caas.cn (M.Z.); zhanglijiao@caas.cn (L.Z.)

³ Key Laboratory of Microbial Resources, Ministry of Agriculture and Rural Affairs, Beijing 100081, China

* Correspondence: wuxiangli@caas.cn

Abstract: *Pleurotus ostreatus* is one of the most cultivated edible mushrooms worldwide, of which the fruiting body development is a highly complex process involving the precise genetic regulatory network and suitable environmental factors. Metacaspases play important roles in developmental processes and programmed cell death (PCD) induced by some environmental stress in many organisms. In this study, a type I metacaspase, *PoMCA1*, was identified via the analysis of the enzyme domain and alignment with homologous metacaspases. *PoMCA1* overexpression and RNAi mutants were generated via *Agrobacterium tumefaciens*-mediated transformation (ATMT) into the *P. ostreatus* mycelium. The roles of the *PoMCA1* gene in heat stress and fruiting body development were examined. The results show that both of the overexpression transformants were more tolerant to heat stress than the wild-type strain, while the opposite phenomena were found for the two RNAi strains. Compared with the wild-type strain, the overexpression strain OE-7 had faster formation of the fruiting body, while the two RNAi strains produced significantly more primordia and young fruiting bodies, and presented morphological deformities and slower fruiting body development. All of the results suggest that the *PoMCA1* gene is involved in the positive regulation of heat stress tolerance and fruiting body development in *P. ostreatus*.

Keywords: fruiting body development; genetic transformation; heat stress; metacaspase; *Pleurotus ostreatus*; qRT-PCR



Citation: Pei, J.; Zhao, M.; Zhang, L.; Wu, X. The Metacaspase Gene *PoMCA1* Enhances the Mycelial Heat Stress Tolerance and Regulates the Fruiting Body Development of *Pleurotus ostreatus*. *Horticulturae* **2024**, *10*, 116. <https://doi.org/10.3390/horticulturae10020116>

Academic Editor: Mingwen Zhao

Received: 30 December 2023

Revised: 20 January 2024

Accepted: 21 January 2024

Published: 24 January 2024



Copyright: © 2024 by the authors. Licensee MDPI, Basel, Switzerland. This article is an open access article distributed under the terms and conditions of the Creative Commons Attribution (CC BY) license (<https://creativecommons.org/licenses/by/4.0/>).

1. Introduction

Pleurotus ostreatus, also known as oyster mushroom, is widely cultivated all over the world and especially in China. It is rich in essential amino acids, a variety of trace elements, and bioactive components, which have potential applications in health care and medical industries [1,2]. The development of *P. ostreatus* from mycelium to primordium, young fruiting body, and mature fruiting body sequentially is a highly complex process, which involves a precise genetic regulatory network and suitable environmental factors, such as humidity, carbon dioxide concentration, and especially temperature. The study on the molecular mechanisms of fruiting body development will be beneficial to our fundamental understanding of the formation of mushroom yield and quality, so as to effectively guide cultivation. In recent years, *P. ostreatus* has become a potentially good model system for elucidating physiological and biochemical processes in basidiomycota, and genetic tools including gene silencing, overexpression, and efficient genetic transformation systems [3], have been applied to *P. ostreatus*, providing more possibilities for exploring the functions of target genes. Some genes have been found to play roles in fruiting body development

and stress response. For example, disruption of *pal1*, which encodes the phenylalanine ammonia-lyase (*pal*) in *P. ostreatus*, resulted in heat tolerance, whereas disruption of the other *pal* gene, *pal2*, led to tolerance to H₂O₂ [4]. The superoxide dismutase (SOD)-overexpressing strains OE-*Mnsod1-1* and OE-*Mnsod1-21* shortened the mycelial recovery time after heat stress in *P. ostreatus* [5]. Catalase (CAT) also affected the development of *P. ostreatus*, and primordial differentiation was blocked in *cat1*-overexpressing strains [6]. Silenced strains of *Pofst3*, the homologous transcription factor for *fst3* in *Schizophyllum commune*, formed more primordia and smaller fruiting bodies than wild-type strains of *P. ostreatus* [7].

Cysteine proteases are widely involved in cellular differentiation and degradation, and play important roles in PCD processes in animals, plants, and microorganisms [8]. Aspartate-specific cysteine proteases (caspases), widely found in metazoans, are a subfamily of cysteine proteases. However, the cysteine proteases in protozoan [9–11], fungi [12], and plants [13] share some sequence and three-dimensional structural similarities with caspases but lack aspartate specificity, and thus were called metacaspases [14]. Metacaspases can be categorized based on primary sequence similarity and the predicted structure of tertiary domains into three types: type I, type II, and type III. All three types contain highly conserved caspase-like catalytic domains consisting of putative large (p20) and small (p10) subunits, with the presence of the His–Cys catalytic dichotomy required for peptide bond hydrolysis at p20. The catalytic histidine is located in the (H/Y)(Y/F)SGHG sequence and the catalytic cysteine is located in the D(A/S)C(H/Y)S sequence [15]. Type I metacaspases have the presence or absence of a proline-rich N-terminal pre-structural domain. Type II metacaspases lack this pro-structural domain, but have a longer linkage region than type I between the p20 and p10 subunits. The genomes of multicellular organisms usually encode type I and type II cysteine-like enzymes, whereas type III has only been found in a few organisms [16]. Currently, only type I metacaspases are found in protozoan and fungi [17]. Metacaspases are always actively involved in programmed cell death (PCD), which often occurs in different cells in response to a wide variety of stimuli. Overexpression of the metacaspase *Yca1* increased the incidence of apoptosis-like cell death in *Saccharomyces cerevisiae* during oxidative stress and senescence, while the opposite result was observed after interference of the gene [12]. Deletion of metacaspases *PaMCA1* or *PaMCA2* of the filamentous fungus *Podospira anserina* resulted in lifespan extension [18]. Similarly, the type II metacaspase *LcMCII-1* in the woody fruit tree *Litchi chinensis* has the same function [19]. Overexpression of both the *Leishmania major* metacaspase *LmjMCA* and *Trypanosoma cruzi* *TcMCA5* increased sensitivity to stress [20,21]. These studies revealed that metacaspases have pro-death functions, but the cytoprotective function of metacaspases has also been reported in some organisms recently. A previous study in *Aspergillus fumigatus* found that the metacaspases *CasA* and *CasB* promoted growth under endoplasmic reticulum stress [22]. The metacaspase *mcII-Pa* in the embryos of *Norway spruce* has a pro-survival role at the early stages of cell death [23]. The metacaspase *TcMCA3* in *T. cruzi* played roles in the cell cycle and in preventing natural cell death [20]. These findings suggest that metacaspases, with two opposite functions including pro-death and pro-survival, play important roles in biotic and abiotic stresses as well as in developmental processes.

A previous study of our group found that the zinc finger transcription factor *PoZCP26* promoted the development of the primordium and fruiting body of *P. ostreatus* (unpublished). By analyzing the transcriptome data and verified qRT-PCR results of wild-type and *PoZCP26*-RNAi mutants at various developmental stages, a metacaspase-encoding gene, *PoMCA1*, whose expression was up-regulated four-fold in the wild-type strain but was down-regulated by 52–89% in *PoZCP26*-RNAi mutants from the mycelium to primordium developmental stages (Figure S1), was screened out and was assumed to be regulated by *PoZCP26* and be involved in the development of the fruiting body. In this study, we constructed *PoMCA1* overexpression and RNAi strains via *Agrobacterium tumefaciens*-mediated transformation (ATMT) to investigate the roles of this gene in heat stress and the development of *P. ostreatus*. The phenotypic changes of *PoMCA1* transformants will help to elucidate its function in *P. ostreatus*.

2. Materials and Methods

2.1. Strains and Media

P. ostreatus strain CCMSSC00389, provided by the China Center for Mushroom Spawn Standards and Control (CCMSSC), was used as a wild-type strain in this study and was the recipient strain for overexpression and RNAi. The *P. ostreatus* wild-type strain and transformants were all cultured on potato dextrose agar medium (PDA: 39 g/L of Difco™ potato dextrose agar, 2.5 g/L of agar; BD, Sparks, MD, USA) unless otherwise specified. The *Escherichia coli* DH5 α (Genesand, Beijing, China) strain was used for cloning and plasmid propagation, and the *A. tumefaciens* strain GV3101 (preserved in our lab) was used to transfer the plasmid into the *P. ostreatus* mycelium. To produce fruiting bodies, the mushroom strains were cultured in tissue culture bottles containing cultivation medium (94% cottonseed hulls, 5% wheat bran, and 1% lime) with 65% water content.

2.2. Gene Structure and Protein Properties Analysis

The *PoMCA1* gene sequence was obtained from the genome of the *P. ostreatus* strain CCMSSC00389 (NCBI accession number GCA_001956935.2). Sequencing was performed after ligating the cloned *PoMCA1* gene into the cloning vector pEASY-Blunt Zero. After comparison with the genomic *PoMCA1* sequence on NCBI, the verified sequence was uploaded to NCBI with the accession number (PPO01696). The gene structure of *PoMCA1* was analyzed using GSDS (Gene Structure Display Server 2.0). Euk-mPLoc2.0 (<http://www.csbio.sjtu.edu.cn/bioinf/euk-multi-2/>, accessed on 20 July 2023) was used for subcellular localization analysis and InterPro (<http://www.ebi.ac.uk/interpro>, accessed on 21 January 2024) was adopted for protein structural domain prediction.

2.3. Phylogenetic Analysis and Multiple Sequence Alignment

Multiple sequence alignment among *PoMCA1* and metacaspases from various fungi, plants, and protozoa was performed using Jalview 2.11.3.2. Phylogenetic trees were constructed using MEGA 11. To assess the statistical reliability of each node, bootstrap analyses were performed with 1000 replications using the maximum likelihood algorithm.

2.4. DNA/RNA Extraction and cDNA Synthesis

Total genomic DNA (gDNA) and total RNA were extracted from the mycelia of *P. ostreatus*, which had been cultured on PDA medium at 28 °C for 5 days, using the Plant Genomic DNA Extraction Kit (Tiangen, Beijing, China) and the Plant RNA Extraction Kit (Omega, Norcross, GA, USA), respectively, according to the manufacturers' protocols. The cDNA was synthesized from RNA using the HiScript III 1st Strand cDNA Synthesis Kit (+gDNA wiper) (Vazyme, Nanjing, China).

2.5. Gene Cloning and Plasmids Construction

The fragments of *PoMCA1* were cloned using total gDNA and cDNA as templates. All of the primers are listed in Table S1. The PCR reaction system with a total of 25 μ L included 1 μ L of template, 12.5 μ L of 2 \times Phanta Max Master Mix, 1 μ L of *PoMCA1*-F primer, 1 μ L of *PoMCA1*-R primer, and 9.5 μ L of ddH₂O. The amplification program was set as follows: 95 °C for 3 min; 34 cycles of 95 °C for 30 s, 58 °C for 30 s, and 72 °C for 45 s; and 72 °C for 5 min. The PCR products were purified using the FastPure Gel DNA Extraction Mini Kit (Vazyme, Nanjing, China) and were cloned into the pEASY-Blunt Zero Cloning Vector and transformed into *E. coli* DH5 α -competent cells. The kanamycin-resistant colonies were picked for sequencing and the generated vectors containing correct gDNA or cDNA sequences of *PoMCA1* were used as templates in the following PCR.

The vector Po-gpdOE, constructed in our lab [3], was used as the initial vector to construct *PoMCA1* overexpression and RNAi plasmids. To construct the *PoMCA1* overexpression vector, the coding region of the *PoMCA1* gene was amplified using PCR with the OE-*PoMCA1* F/R primers harboring vector homology arms. The initial Po-gpdOE vector was digested with *Bam*HI (NEB, Ipswich, MA, USA) and *Xba*I (NEB, Ipswich, MA, USA),

and then the purified *PoMCA1*-coding fragment was ligated into the vector via homologous recombination using the ClonExpress[®] II One Step Cloning Kit (Vazyme, Nanjing, China). The fragment covering 81 bp to 496 bp of the *PoMCA1* cDNA was selected as the interference target, and the primers Ri-sense-*PoMCA1* F/R and Ri-anti-*PoMCA1* F/R containing vector homology arms were designed to amplify the sense and antisense fragments interrupted by a 60 bp spacer fragment. The purified fragments were successively ligated to *Po*-gpdOE via homologous recombination and the RNAi vector was generated.

2.6. *A. tumefaciens* Mediated Transformation (ATMT) into *P. ostreatus* Mycelia

The constructed *PoMCA1* overexpression and RNAi plasmids were transformed into *E. coli* DH5 α for cloning, sequencing, and plasmid propagation. The verified overexpression plasmid *Po*-gpdOE-*PoMCA1* and the RNAi plasmid RNAi-*PoMCA1* were transformed into the *P. ostreatus* wild-type strain using the ATMT method described before [4].

To confirm the integration of the target gene fragments into the wild-type genome, the gDNAs of the transformants were used as the templates to amplify the gene hygromycin B phosphotransferase fragment (Hyg) via PCR using the primer Hyg-F/R.

2.7. Quantitative Real-Time Reverse-Transcription PCR (qRT-PCR)

The expression of *PoMCA1* in the wild-type strain and transformants was verified using qRT-PCR. The α -tubulin was used as the reference gene. Each qRT-PCR reaction mixture of 10 μ L contained 0.2 μ L of 10 μ M primer, 5 μ L of Taq Pro Universal SYBR qPCR Master Mix (Vazyme, Nanjing, China), 1 μ L of cDNA template, and 3.6 μ L of ddH₂O. The reaction program was set as follows: 95 $^{\circ}$ C for 30 s, followed by 40 cycles of 95 $^{\circ}$ C for 10 s and 60 $^{\circ}$ C for 30 s. The relative expression level was calculated according to the equation $2^{-\Delta\Delta C_t}$. Three technical replicates and three biological replicates were performed for each sample.

2.8. Determination of Mycelial Growth Rate (MGR)

The mycelial growth rate (MGR) was tested both on PDA and in cultivation medium. For the test on PDA, all of the plates were incubated in the dark at 28 $^{\circ}$ C for 4 d. The diameter of the mycelial radial colony was measured in two perpendicular directions crossed at the mycelial disc and the MGR on PDA was denoted by the radial growing length per day. The MGR assay in the cultivation medium was performed in 30 \times 200 mm test tubes. Mycelial discs (5 mm diameter) were inoculated onto the medium and incubated in the dark at 28 $^{\circ}$ C. The distance from the end point of growing mycelia to the start point was measured at different time intervals. The MGR in cultivation medium was calculated as the mycelia growing length along the tube per day. All of the experiments were performed in triplicate and repeated three times.

2.9. Heat Stress Treatment

All of the wild-type and transformant strains were cultured on PDA plates at 28 $^{\circ}$ C for 4 days and then subjected to 35 $^{\circ}$ C and 40 $^{\circ}$ C for 48 h, respectively. Then, the plates were placed back at 28 $^{\circ}$ C for 2 and 3 days of recovery, respectively. The diameters of mycelial radial colonies before and after heat stress were measured. The strains without heat stress treatment were set as respective controls for each strain. The mycelial growth inhibition rate (MGIR) was calculated as $(D_c - D_t)/D_c \times 100\%$ (D_c = average diameter of radial growth in the control; D_t = average diameter of radial growth during heat stress treatment). The mycelial recovery growth rate (MRGR) was calculated as the mycelial growth rate during recovery.

2.10. Fruiting Body Cultivation and Phenotypic Analysis of Transformants

All of the strains were inoculated to the cultivation medium and incubated at 28 $^{\circ}$ C. When the spawn running was finished, the cultured bottles were placed in an artificial climate chamber to produce fruiting bodies. The formation time for various stages and

the number of young fruiting bodies were recorded or photographed. To measure spore production, the mature fruiting bodies were taken and spores were collected and counted with a hemocytometer (Corning, NY, USA). The cultivation experiment was performed twice with 10 bottles for each strain each time.

2.11. Statistical Analysis

All of the experiments described in this study were performed in three independent replications unless otherwise specified. Error bars indicate the standard deviations (SD) of the three replicated samples. Statistical analysis and one-way ANOVA were performed using SPSS 17.0. Differences were considered statistically significant at $p < 0.05$.

3. Results

3.1. Identification of *PoMCA1* from *P. ostreatus*

The *PoMCA1* gene, with a length of 1938 bp, contains 14 exons and 13 introns, and encodes a protein including 395 amino acid residues (Figure 1A). Subcellular localization analysis showed that the protein mainly functions in the cytoplasm. Protein domain analysis revealed that the *PoMCA1* protein contains a conserved functional domain named peptidase C14, which belongs to the caspase-like superfamily (Figure 1B). Some reported type I and type II metacaspases were selected to perform the phylogenetic analysis, which showed that *PoMCA1* was clustered in the type I metacaspase branch (Figure 2), suggesting that *PoMCA1* is a type I metacaspase.

3.2. Multiple Sequence Alignment

The *PoMCA1* protein was used for alignment with type I metacaspases from *Arabidopsis thaliana*, *Trypanosoma brucei*, *A. fumigatus*, *Aspergillus nidulans*, *S. cerevisiae*, and *Schizosaccharomyces pombe*, and the results revealed conserved motifs and structural features of the metacaspases (Figure 3). All of the metacaspases have a conserved caspase-like structural domain consisting of a p20 subunit containing a caspase-specific catalytic dyad of His–Cys, a linker region, and a p10 subunit. *PoMCA1* has structural similarity to the known type I metacaspases described above, with a short linkage region between the p20 and p10 subunits (Figure 3), which characterizes a type I metacaspase. Therefore, *PoMCA1* was considered as a type I metacaspase.

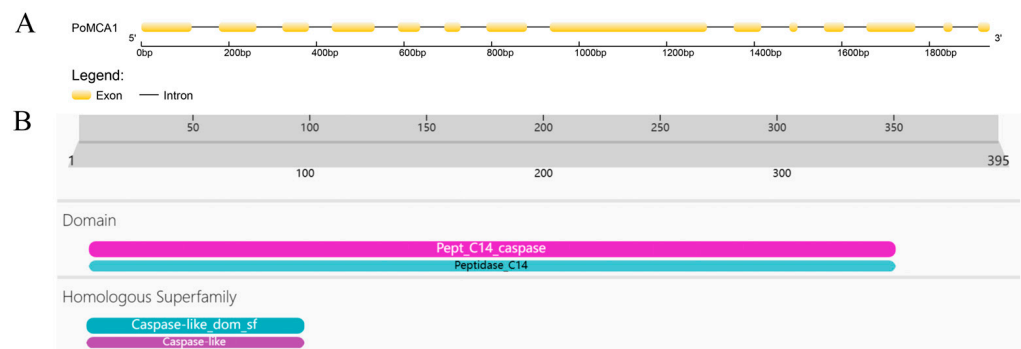


Figure 1. Gene structure and protein domain of *PoMCA1*. (A) Gene structure. (B) Protein domain.

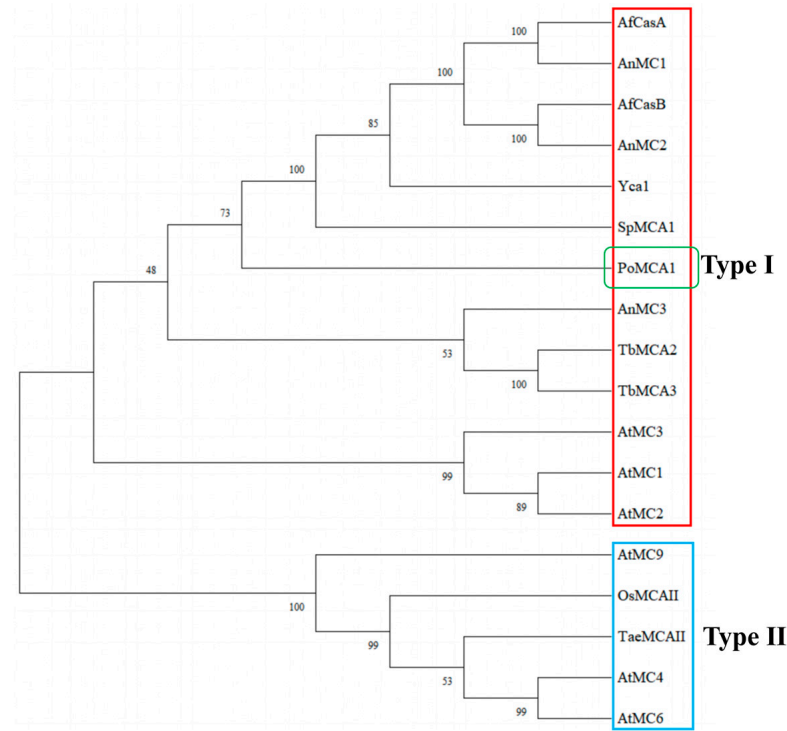


Figure 2. Neighbor-joining phylogenetic tree of type I (red box) and type II metacaspases (blue box). Amino acid sequences were from *Arabidopsis thaliana* (AtMC1 AEE27396.1, AtMC2 AEE85012.1, AtMC3 AED97859.1, AtMC4 AEE36232.1, AtMC6 AEE36230.1, AtMC9 AED90710.1), *Oryza sativa* L. (OsMCAII AAT07577.1), *Triticum aestivum* (TaeMCAII ACY82389.1), *T. brucei* (TbMCA2 AAX80349.1, TbMCA3 AAX80348.1), *A. fumigatus* (AfCasA XP_750419.2, AfCasB EAL92173.1), *A. nidulans* (AnMC1 AAO13381.1, AnMC2 CBF86986.1, AnMC3 CBF75174.1), *S. cerevisiae* (Yca1 AAT92851.1), and *S. pombe* (SpMCA1 O74477.1). The metacaspase *PoMCA1* in *P. ostreatus* was highlighted in the green box. The value at the branch point is the bootstrap of the phylogenetic tree.



Figure 3. Sequence alignment of *PoMCA1* from *P. ostreatus* and the metacaspases from *A. fumigatus* AfCasA (XP_750419.2) and AfCasB (EAL92173.1); *A. nidulans* AnMC1 (AAO13381.1), AnMC2(CBF86986.1), AnMC3(CBF75174.1); *S. cerevisiae* Yca1(AAT92851.1); *S. pombe* SpMCA1(O74477.1); *T. brucei* TbMCA2(AAX80349.1), and TbMCA3 (AAX80348.1). *A. thaliana* AtMC1 (AEE27396.1), AtMC2 (AEE85012.1), AtMC3 (AED97859.1); the p20-like and p10-like regions are outlined with black and red, respectively. Active sites are denoted with asterisks. The capital letters in the different background colors denote conserved amino acids.

3.3. Generation of Overexpression and Interference Transformants

The DNA and cDNA of the *PoMCA1* protein were obtained via PCR, with the fragment sizes of 1938 bp and 1188 bp, respectively (Figure S2A,B). The coding DNA sequence (CDS) region and gene interference fragments (sense, loop, and antisense) of the *PoMCA1* protein were ligated with the linear vector, *Po-gpdOE*, and *PoMCA1* overexpression and RNAi vectors were constructed successfully. The schematic diagrams of both vectors are shown in Figure S3.

PoMCA1 overexpression and RNAi vectors were successfully transferred into *P. ostreatus* via ATMT. *PoMCA1* overexpression and RNAi transformants resistant to hygromycin were screened out and were PCR-amplified using Hyg-F/R primers. The results of the PCR assay showed that Hyg fragments were detected in the genomes of most of the OE and RNAi transformants, suggesting that the vector fragments containing the target gene were all successfully integrated into the genome of these transformants (Figure S4A,B). Five positive OE and RNAi transformants were selected to examine the expression of *PoMCA1* via qRT-PCR. The expression levels of *PoMCA1* in the overexpression strains were up-regulated by about 3–4 fold (Figure 4A), and that in the RNAi strains was reduced by about 50–65% (Figure 4B). Through comprehensively evaluating the resistance of transformants to hygromycin and the relative expression level of *PoMCA1* after successive subculturing, the overexpression strains OE-2 and OE-7 and the RNAi strains Ri-25 and Ri-33 were selected for the subsequent experiments.

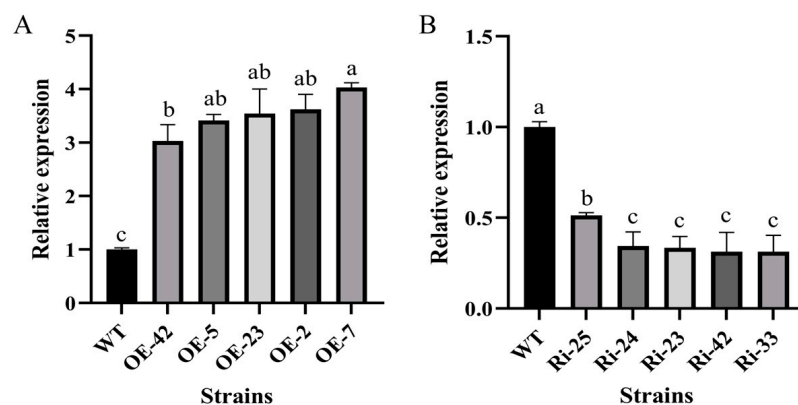


Figure 4. The relative expression levels of *PoMCA1* in *P. ostreatus* transformants. (A) OE transformants; (B) RNAi transformants. WT: wild-type. Different letters indicate significant differences among strains at $p < 0.05$.

3.4. *PoMCA1* Promoted Mycelial Growth and Heat Resistance on PDA

The mycelial growth experiment on PDA plates at 28 °C showed that the two RNAi strains grew much more slowly than the WT (Figure 5A) and the MGRs of both RNAi strains were significantly reduced compared to the WT (Figure 5D). Contrarily, the MGR of the overexpression strain OE-7 was significantly higher than that of the WT (Figure 5D). The results indicate that *PoMCA1* positively regulated the growth of the mycelium.

During the heat treatment at 35 °C for 2 days, the MGIRs of the overexpression strains OE-2 and OE-7 were found to be significantly lower than that of the WT, but the MGIR of RNAi strain Ri25 was significantly higher than that of the WT. Although there were no significant differences in the MRGR for all the strains during the recovery period (data not shown), the colony edges of both RNAi strains were more irregular and sparse than other strains (Figure 5B,E). These results suggest that the *PoMCA1* gene enhanced mycelial tolerance under moderate high temperature (35 °C) treatment and determined the morphology of the mycelium to some extent.

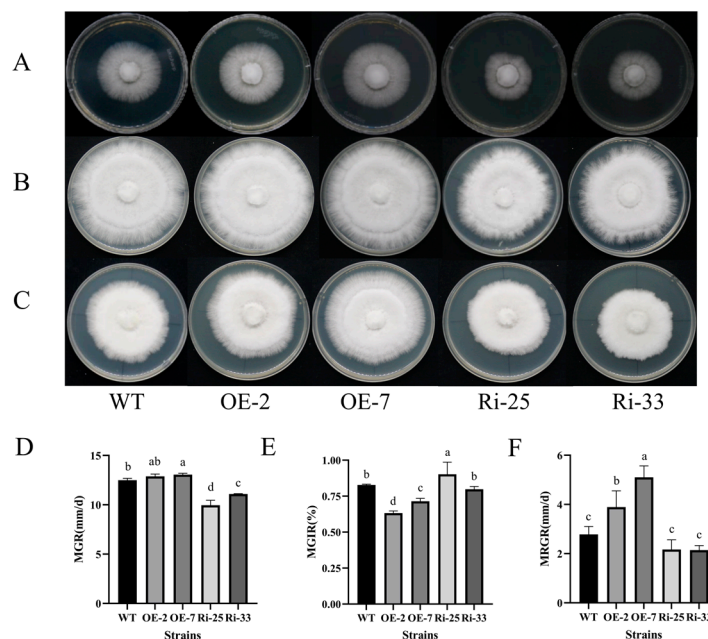


Figure 5. Normal growth and heat resistance of wild-type strain and transformant mycelia on the PDA medium. (A) Colony morphology of wild-type strain and transformants cultured at 28 °C for 4 days. (B) Colony morphology of wild-type strain and transformants recovered at 28 °C for 2 days after 4 days of culturing at 28 °C and 2 days of heat treatment at 35 °C. (C) Colony morphology of wild-type strain and transformants recovered at 28 °C for 3 days after 4 days of culturing at 28 °C and 2 days of heat treatment at 40 °C. (D) The MGRs of wild-type strain and transformants cultured at 28 °C for 4 days. (E) The MGIRs of wild-type strain and transformants cultured at 28 °C for 4 days and heat stressed at 35 °C for 2 days. (F) The MRGRs recovered for 3 days after 4 days of culturing at 28 °C and 2 days of heat stress at 40 °C. Different lowercase letters indicate significant differences between the analyzed samples ($p < 0.05$).

When heat stressed at 40 °C for 2 days, the mycelia of the WT and transformants all stopped growing. During the recovery at 28 °C, the growth of RNAi strains was severely affected and the MRGRs of the RNAi strains were significantly lower, while those of the overexpression strains were significantly higher than those of the WT (Figure 5C,F). The results revealed that the *PoMCA1* gene positively regulated the mycelia to recover its growth after extreme high temperature (40 °C) treatment.

3.5. *PoMCA1* Regulated the Fruiting Body Development

The MGRs assay in the cultivation medium showed that all of the strains had similar MGR curves with a trend of a sharp to moderate increase (Figure 6A). During the first seven days of colonization, the MGRs of the overexpression strains were significantly higher, while those of the RNAi strains were significantly lower compared to the wild-type strain (Figure 6B). The results indicate that the *PoMCA1* gene promoted mycelial growth and especially colonization in the cultivation medium.

Cultivation of the fruiting body was performed for the wild-type, overexpression, and RNAi strains. There were no significant time differences in the formation of the primodium among all strains (Figure 7A), while the fruiting body formation of both RNAi strains was significantly postponed relative to that of the wild-type (Figure 7B). When cultured for the same period of time, the wild-type and overexpression strains were already mature, while the RNAi strains were still in the period of young mushrooms (Figure S5), and the RNAi strains produced a significantly larger number of young mushrooms than the wild-type strains (Figures 7C and 8). The cap morphology of the wild-type and overexpression strains was nearly round at the time of the fruiting body maturation, while that of both RNAi strains was irregular (Figure 8). The results indicate that the *PoMCA1* gene

accelerated the developmental rate, controlled the primordia within a certain amount and promoted the normal differentiation of the cap in *P. ostreatus*. Afterwards, spore production was examined, and the overexpression strain OE-2 had significantly fewer spores, while the RNAi strains had significantly more spores than the wild-type strain (Figure 9). This suggested that the *PoMCA1* gene limited the spore production of *P. ostreatus* to some extent.

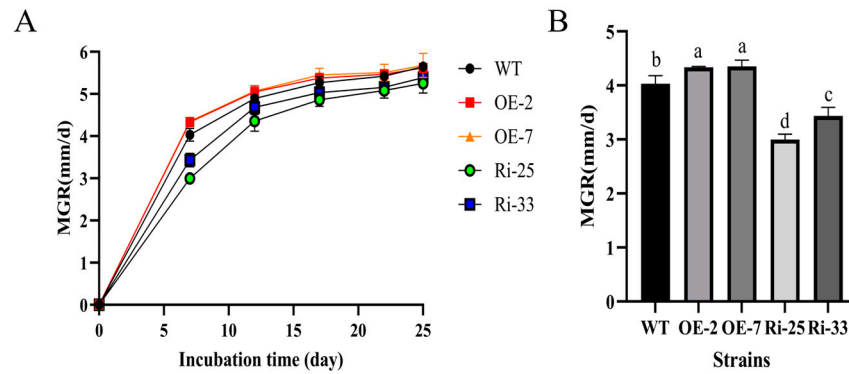


Figure 6. MGRs tested in cultivation medium. (A) The MGR curves. (B) The MGRs at day 7 of incubation. Different lowercase letters indicate significant differences between the analyzed samples ($p < 0.05$).

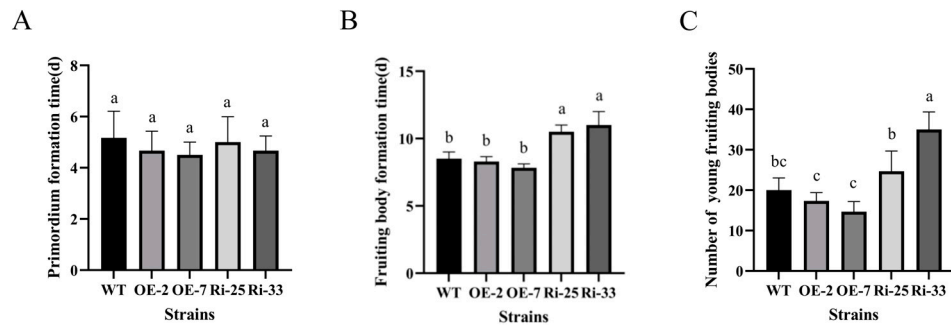


Figure 7. Characteristics of fruiting body formation of the wild-type strain and transformants. (A) Primordium formation time; (B) fruiting body formation time; (C) number of young fruiting bodies. Different lowercase letters indicate significant differences among strains at $p < 0.05$.

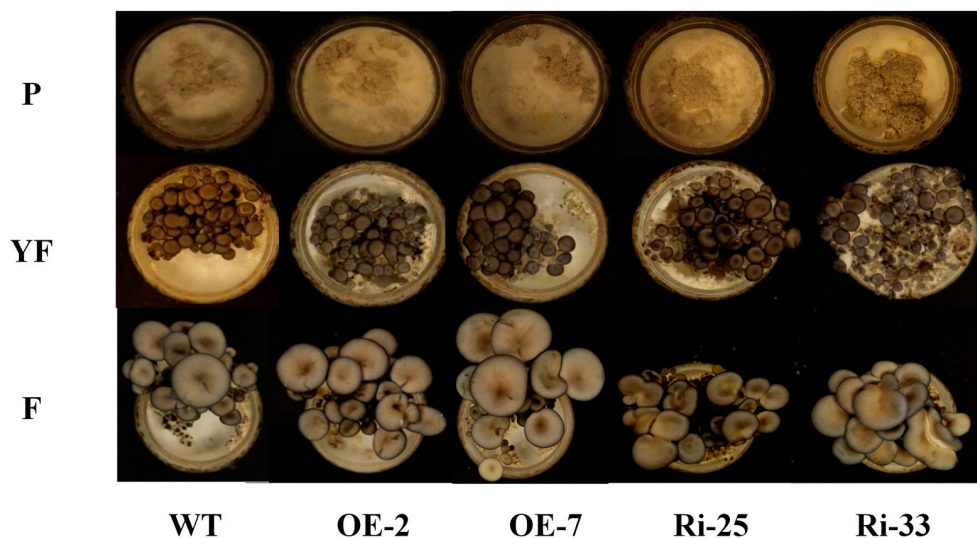


Figure 8. Fruiting body development of the wild-type strain and transformants. P: primordium; YF: young fruiting body; F: mature fruiting body.

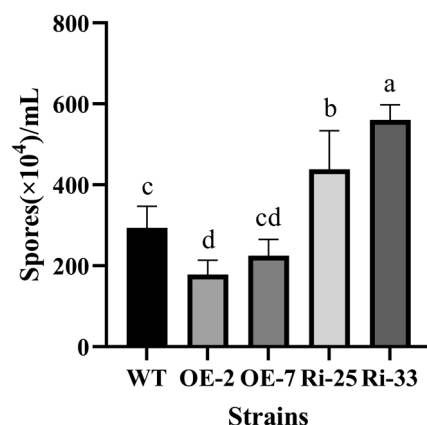


Figure 9. Spore numbers of wild-type stain and transformants. Different lowercase letters indicate significant differences between the analyzed samples ($p < 0.05$).

4. Discussion

Metacaspases are cysteine-dependent proteases found in protozoa, fungi, and plants. Metacaspases have a varying number of family members in different species, and genome-wide characterizations of the metacaspase gene family have been reported in several plant species, including *A. thaliana* [24], grape [25], rice [26], rubber [27], tomato [28], and potato [29]. Although metacaspases have been extensively studied in plants, functional identifications in edible mushrooms have not been reported. Transcriptomic data showed that the expression of *PoMCA1* in *P. ostreatus* was stage-specific and developmentally regulated (Figure S1). The phylogenetic tree showed that *PoMCA1* has the highest homology with a type I metacaspase SpMCA1 from *S. pombe* and is clustered in type I (Figure 2). Multiple sequence alignment results revealed that they had similar structures (Figure 3), further suggesting that *PoMCA1* encodes a metacaspase. Thus, we studied the role of the metacaspase gene *PoMCA1* in *P. ostreatus*.

Metacaspases have been shown to be developmentally and spatially regulated and to be involved in a variety of defense responses under biotic and abiotic stresses. Some metacaspases played protective roles in stress response. For example, in the filamentous ascomycete *A. fumigatus*, deletion mutants of two metaspase genes, *CasA* and *CasB*, showed a growth detriment in endoplasmic reticulum (ER) stress [22]. The *S. pombe* metacaspase acted as a cellular protector in response to cadmium-induced oxidative stress [30]. The cultivation quality of *P. ostreatus* is closely related to the temperature of the natural environment, and high temperature, the adverse effects of which can cause great economic losses, is the most unfavorable stress in the cultivation of *P. ostreatus* [31], so it is necessary to study the mechanism of resistance to heat stress in *P. ostreatus*. Our study demonstrated the role of the metacaspase in the response to heat stress in *P. ostreatus*. Overexpression of *PoMCA1* enhanced mycelial tolerance to heat stress, positively regulated the ability of mycelia to resume growth after heat stress, and influenced the morphology of the mycelia to a certain extent (Figure 5B,C,E,F), which implies that *PoMCA1* has a specific cytoprotective role in response to heat stress. These results correspond to those previous reports. However, many reports indicated that metacaspase is a key enzyme involved in the PCD process. For instance, *AtMC4* in *A. thaliana* positively regulated cell death triggered by biotic and abiotic stresses [32]. Overexpression of *Camc9* in pepper caused programmed cell death when infected with bacterial pathogens [33]. Besides the roles involved in stress, metacaspases were also reported to have cytoprotective functions. Deletion of the two metacaspase genes in the filamentous fungus *P. anserina* resulted in slower growth rates and affected reproductive capacity, suggesting that the metacaspases played important roles in its development [18]. The metacaspase of *S. pombe*, in addition to its role in oxidative stress response, also promoted its cell growth [30]. Similarly in our study, mycelial growth rate assays performed either on PDA plates or in cultivation medium showed that *PoMCA1* promoted

the mycelial growth (Figures 5A,D and 6). These reports revealed that the metacaspases have both pro-death and pro-survival functions.

In recent years, the mechanism of fruiting body formation has become a research hotspot. In the present study, it was discovered that the *PoMCA1* RNAi strains formed more primordia and young fruiting bodies than the wild-type strains (Figures 7C and 8), which might in turn have led to slow development and malformed fruiting bodies (Figures 7B, 8 and S5). These results suggest that the metacaspase plays an important role in the process of the fruiting body development of *P. ostreatus*. We suppose that the metacaspase encoded by the *PoMCA1* gene might activate cell apoptosis to maintain a moderate number of fruiting bodies, and thus to ensure normal growth and development. Previous reports revealed that PCD-like processes were involved in tissue differentiation [34] and spore production [35]. It was found in our study that the overexpression strain OE-2 produced significantly less spores than the wild-type strain, while the amount of spores significantly increased after gene disruption of *PoMCA1* (Figure 9). By contrast, spore production was reduced in *Magnaporthe oryzae* with simultaneous mutations of *MoMca1* and *MoMca2* [36]. However, both the deletion of the apoptosis suppressor gene *FpBIR1* and the deletion of apoptosis inducer gene *FpNUC1* in *Fusarium pseudograminearum* produced fewer conidia [37]. These observations reinforce the fact that the functions of metacaspases are complicated and various in different organisms. These results clearly indicate that the gene *PoMCA1* encoding metacaspases in *P. ostreatus* plays an important regulatory role in the formation of the fruiting body; however, the involved regulatory mechanisms in these processes are still not clear. Therefore, further researches on *PoMCA1* are needed to elucidate the molecular mechanisms of its regulation in abiotic stress tolerance and the fruiting body development.

5. Conclusions

In this study, we identified and characterized a type I metacaspase gene, *PoMCA1*, in *P. ostreatus*. We constructed the overexpression and RNAi mutants of *PoMCA1* and studied its role in the heat stress response and the growth development of the fruiting body. The results show that it enhanced the heat tolerance, accelerated the developmental rate, controlled the primordia and spores within a certain amount, and promoted the normal differentiation of the cap in *P. ostreatus*. The study discovered new genes regulating the heat stress response and development of *P. ostreatus* and thus laid the foundation for further research on the function of metacaspases.

Supplementary Materials: The following supporting information can be downloaded at: <https://www.mdpi.com/article/10.3390/horticulturae10020116/s1>. Figure S1: *PoMCA1* expression between wild-type and *PoZCP26* RNAi strains from mycelia (M) to the primordium (P) stage. Black: RNA-seq; red: qRT-PCR. Figure S2: PCR amplification of *PoMCA1* DNA and CDS. (A) DNA; (B) CDS. M: Vazyme Marker DL5000bp; 1: DNA 1938 bp; 2: CDS 1188bp. Figure S3: The plasmid maps. (A) *Po-gpdOE-PoMCA1*. (B) *RNAi-PoMCA1*. Figure S4: PCR amplification of the hygromycin B phosphotransferase fragment from the genome DNA of putative transformants. (A) Overexpression; (B) RNAi. M: Vazyme Marker DL2000; Lane 1–21: putative *PoMCA1* transformants; CK: positive control (*PoMCA1* overexpression/RNAi plasmid); NC1: negative control (wild-type); NC2: negative control (ddH₂O). Figure S5: The phenotype of the fruiting bodies of wild-type strains and transformants on the 28th day (from the time of inoculation). Table S1: List of primers used in this study.

Author Contributions: J.P. participated in all experimental procedures and drafted the manuscript; M.Z. participated in the analysis of the data; L.Z. participated in mushroom cultivation; X.W. proposed research topics, designed research programs, supervised the study, and critically revised the manuscript. All authors have read and agreed to the published version of the manuscript.

Funding: This research was funded by the National Natural Science Foundation of China (32072643) and the Fundamental Research Funds for the China Agriculture Research System (CARS20).

Data Availability Statement: Data are contained within the article or Supplementary Materials.

Conflicts of Interest: The authors declare no conflicts of interest.

References

- Shen, J.; Liu, C.; Zhang, Q.; Li, J.; Qi, Y.; Qiu, L.; Gao, Y.; Wen, Q. Effect of five different cultivation substrates on nutrients in fruiting body of *Pleurotus ostreatus*. *J. Henan Agric. Sci.* **2016**, *45*, 103–106.
- Wen, Q.; Zhu, L.; Yu, H.; Chen, H.; Li, J.; Shen, J. Effects of spent mushroom substrate and nutritional component of factory-cultivated *Flammulina velutipes* on the sterilized raw material cultivation and nutritional component of *Pleurotus ostreatus*. *North. Hortic.* **2021**, *02*, 124–130.
- Lei, M.; Wu, X.; Zhang, J.; Wang, H.; Huang, C. Establishment of an efficient transformation system for *Pleurotus ostreatus*. *World J. Microbiol. Biotechnol.* **2017**, *33*, 214. [[CrossRef](#)] [[PubMed](#)]
- Hou, L.; Wang, L.; Wu, X.; Gao, W.; Zhang, J.; Huang, C. Expression patterns of two *pal* genes of *Pleurotus ostreatus* across developmental stages and under heat stress. *BMC Microbiol.* **2019**, *19*, 231. [[CrossRef](#)] [[PubMed](#)]
- Hou, L.; Liu, Z.; Yan, K.; Xu, L.; Chang, M.; Meng, J. *Mnsod1* promotes the development of *Pleurotus ostreatus* and enhances the tolerance of mycelia to heat stress. *Microb. Cell Fact.* **2022**, *21*, 155. [[CrossRef](#)] [[PubMed](#)]
- Wang, L. Characterization and Function Analysis of Catalase Genes in *Pleurotus ostreatus*. Ph.D. Thesis, Chinese Academy of Agricultural Sciences, Beijing, China, 2019.
- Qi, Y.; Chen, H.; Zhang, M.; Wen, Q.; Qiu, L.; Shen, J. Identification and expression analysis of *Pofst3* suggests a role during *Pleurotus ostreatus* primordia formation. *Fungal Biol.* **2019**, *123*, 200–208. [[CrossRef](#)]
- Aram, L.; Arama, E. Sporoptosis: Sowing the seeds of nuclear destruction. *Dev. Cell* **2012**, *23*, 5–6. [[CrossRef](#)]
- Lee, K.P.; Kim, C.; Landgraf, F.; Apel, K. EXECUTER1- and EXECUTER2-dependent transfer of stress-related signals from the plastid to the nucleus of *Arabidopsis thaliana*. *Proc. Natl. Acad. Sci. USA* **2007**, *104*, 10270–10275. [[CrossRef](#)]
- Mottram, J.C.; Helms, M.J.; Coombs, G.H.; Sajid, M. Clan CD cysteine peptidases of parasitic protozoa. *Trends Parasitol.* **2003**, *19*, 182–187. [[CrossRef](#)]
- Szallies, A.; Kubata, B.K.; Duszenko, M. A metacaspase of *Trypanosoma brucei* causes loss of respiration competence and clonal death in the yeast *Saccharomyces cerevisiae*. *FEBS Lett.* **2002**, *517*, 144–150. [[CrossRef](#)]
- Madeo, F.; Herker, E.; Maldener, C.; Wissing, S.; Lachelt, S.; Herlan, M.; Fehr, M.; Lauber, K.; Sigrist, S.J.; Wesselborg, S.; et al. A caspase-related protease regulates apoptosis in yeast. *Mol. Cell* **2002**, *9*, 911–917. [[CrossRef](#)] [[PubMed](#)]
- Vercammen, D.; van de Cotte, B.; De Jaeger, G.; Eeckhout, D.; Casteels, P.; Vandepoele, K.; Vandenberghe, I.; Van Beeumen, J.; Inze, D.; Van Breusegem, F. Type II metacaspases Atmc4 and Atmc9 of *Arabidopsis thaliana* cleave substrates after arginine and lysine. *J. Biol. Chem.* **2004**, *279*, 45329–45336. [[CrossRef](#)] [[PubMed](#)]
- Uren, A.G.; O'Rourke, K.; Aravind, L.; Pisabarro, M.T.; Seshagiri, S.; Koonin, E.V.; Dixit, V.M. Identification of paracaspases and metacaspases: Two ancient families of caspase-like proteins, one of which plays a key role in MALT lymphoma. *Mol. Cell* **2000**, *6*, 961–967. [[CrossRef](#)] [[PubMed](#)]
- Fagundes, D.; Bohn, B.; Cabreira, C.; Leipelt, F.; Dias, N.; Bodanese-Zanettini, M.H.; Cagliari, A. Caspases in plants: Metacaspase gene family in plant stress responses. *Funct. Integr. Genom.* **2015**, *15*, 639–649. [[CrossRef](#)] [[PubMed](#)]
- Klemencic, M.; Funk, C. Type III metacaspases: Calcium-dependent activity proposes new function for the p10 domain. *New Phytol.* **2018**, *218*, 1179–1191. [[CrossRef](#)]
- Tsiatsiani, L.; Van Breusegem, F.; Gallois, P.; Zavalov, A.; Lam, E.; Bozhkov, P.V. Metacaspases. *Cell Death Differ.* **2011**, *18*, 1279–1288. [[CrossRef](#)]
- Hamann, A.; Brust, D.; Osiewacz, H.D. Deletion of putative apoptosis factors leads to lifespan extension in the fungal ageing model *Podospira anserina*. *Mol. Microbiol.* **2007**, *65*, 948–958. [[CrossRef](#)]
- Wang, C.C.; Lü, P.T.; Zhong, S.L.; Chen, H.B.; Zhou, B.Y. LcMCII-1 is involved in the ROS-dependent senescence of the rudimentary leaves of *Litchi chinensis*. *Plant Cell Rep.* **2017**, *36*, 89–102. [[CrossRef](#)]
- Kosec, G.; Alvarez, V.E.; Aguero, F.; Sanchez, D.; Dolinar, M.; Turk, B.; Turk, V.; Cazzulo, J.J. Metacaspases of *Trypanosoma cruzi*: Possible candidates for programmed cell death mediators. *Mol. Biochem. Parasitol.* **2006**, *145*, 18–28. [[CrossRef](#)]
- Zalila, H.; González, I.J.; El-Fadili, A.K.; Delgado, M.B.; Desponds, C.; Schaff, C.; Fasel, N. Processing of metacaspase into a cytoplasmic catalytic domain mediating cell death in *Leishmania major*. *Mol. Microbiol.* **2011**, *79*, 222–239. [[CrossRef](#)]
- Richie, D.L.; Miley, M.D.; Bhabhra, R.; Robson, G.D.; Rhodes, J.C.; Askew, D.S. The *Aspergillus fumigatus* metacaspases CasA and CasB facilitate growth under conditions of endoplasmic reticulum stress. *Mol. Microbiol.* **2007**, *63*, 591–604. [[CrossRef](#)] [[PubMed](#)]
- Minina, E.A.; Filonova, L.H.; Fukada, K.; Savenkov, E.I.; Gogvadze, V.; Clapham, D.; Sanchez-Vera, V.; Suarez, M.F.; Zhivotovsky, B.; Daniel, G.; et al. Autophagy and metacaspase determine the mode of cell death in plants. *J. Cell Biol.* **2013**, *203*, 917–927. [[CrossRef](#)]
- Kwon, S.I.; Hwang, D.J. Expression analysis of the metacaspase gene family in *Arabidopsis*. *J. Plant Biol.* **2013**, *56*, 391–398. [[CrossRef](#)]
- Zhang, C.; Gong, P.; Wei, R.; Li, S.; Zhang, X.; Yu, Y.; Wang, Y. The metacaspase gene family of *Vitis vinifera* L.: Characterization and differential expression during ovule abortion in stenospermocarpic seedless grapes. *Gene* **2013**, *528*, 267–276. [[CrossRef](#)] [[PubMed](#)]
- Huang, L.; Zhang, H.; Hong, Y.; Liu, S.; Li, D.; Song, F. Stress-responsive expression, subcellular localization and protein-protein interactions of the rice metacaspase family. *Int. J. Mol. Sci.* **2015**, *16*, 16216–16241. [[CrossRef](#)] [[PubMed](#)]
- Liu, H.; Deng, Z.; Chen, J.; Wang, S.; Hao, L.; Li, D. Genome-wide identification and expression analysis of the metacaspase gene family in *Hevea brasiliensis*. *Plant Physiol. Biochem.* **2016**, *105*, 90–101. [[CrossRef](#)] [[PubMed](#)]

28. Liu, H.; Liu, J.; Wei, Y. Identification and analysis of the metacaspase gene family in tomato. *Biochem. Biophys. Res. Commun.* **2016**, *479*, 523–529. [[CrossRef](#)]
29. Dubey, N.; Trivedi, M.; Varsani, S.; Vyas, V.; Farsodia, M.; Singh, S.K. Genome-wide characterization, molecular evolution and expression profiling of the metacaspases in potato (*Solanum tuberosum* L.). *Heliyon* **2019**, *5*, e01162. [[CrossRef](#)]
30. Lim, H.W.; Kim, S.J.; Park, E.H.; Lim, C.J. Overexpression of a metacaspase gene stimulates cell growth and stress response in *Schizosaccharomyces pombe*. *Can. J. Microbiol.* **2007**, *53*, 1016–1023. [[CrossRef](#)]
31. Yan, Z.Y.; Zhao, M.R.; Wu, X.L.; Zhang, J.X. Metabolic response of *Pleurotus ostreatus* to continuous heat stress. *Front. Microbiol.* **2020**, *10*, 3148. [[CrossRef](#)]
32. Watanabe, N.; Lam, E. Arabidopsis metacaspase 2d is a positive mediator of cell death induced during biotic and abiotic stresses. *Plant J.* **2011**, *66*, 969–982. [[CrossRef](#)]
33. Kim, S.M.; Bae, C.; Oh, S.K.; Choi, D. A pepper (*Capsicum annuum* L.) metacaspase 9 (Camc9) plays a role in pathogen-induced cell death in plants. *Mol. Plant Pathol.* **2013**, *14*, 557–566. [[CrossRef](#)] [[PubMed](#)]
34. Umar, M.H.; Van Griensven, L.J.L.D. Morphogenetic cell death in developing primordia of *Agaricus bisporus*. *Mycologia* **1997**, *89*, 274–277. [[CrossRef](#)]
35. Georgiou, C.D. Lipid peroxidation in *Sclerotium rolfisii*: A new look into the mechanism of sclerotial biogenesis in fungi. *Mycol. Res.* **1997**, *101*, 460–464. [[CrossRef](#)]
36. Fernandez, J.; Lopez, V.; Kinch, L.; Pfeifer, M.A.; Gray, H.; Garcia, N.; Grishin, N.V.; Khang, C.H.; Orth, K. Role of two metacaspases in development and pathogenicity of the rice blast fungus *Magnaporthe oryzae*. *mBio* **2021**, *12*, e03471-20. [[CrossRef](#)]
37. Chen, L.L.; Ma, Y.M.; Peng, M.Y.; Chen, W.B.; Xia, H.Q.; Zhao, J.Y.; Zhang, Y.K.; Fan, Z.; Xing, X.P.; Li, H.L. Analysis of apoptosis-related genes reveals that apoptosis functions in conidiation and pathogenesis of *Fusarium pseudograminearum*. *mSphere* **2021**, *6*, e01140-20. [[CrossRef](#)]

Disclaimer/Publisher’s Note: The statements, opinions and data contained in all publications are solely those of the individual author(s) and contributor(s) and not of MDPI and/or the editor(s). MDPI and/or the editor(s) disclaim responsibility for any injury to people or property resulting from any ideas, methods, instructions or products referred to in the content.